Imaging the Himalayan megathrust in northwest India with wave equation migration

Warren B. Caldwell[1], Ashish[2], Jeffrey C. Shragge[1], Shyam S. Rai[2]

[1] Stanford University, Stanford, CA 94305-2215 [2] National Geophysical Research Laboratory, Hyderabad 500 007, India

What is wave-equation migration (WEM)?

Wave-equation migration (WEM) generates images of crustal structure using the scattered coda from seismic waves. It is one of the many imaging techniques in use in the exploration industry. The (non-exhaustive) chart at right illustrates some of the features and assumptions of WEM compared to other common industry imaging approaches.

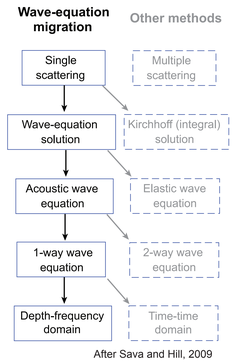

After Sava and Hill, 2009

How does WEM work?

WEM generates images by cross-correlating two seismic wavefields: a source wavefield, and a receiver wavefield containing the scattered coda.

What meant by wavefield?

WEM utilizes the concept of wavefields as multi-dimensional data volumes: for two-dimensional data (i.e. a linear array, such as in this study), the wavefields are represented by a three-dimensional data volume (x,z,t: horizontal distance, depth, and time). The wavefield is a record of the displacements within this volume.

What are the two wavefields?

1. The **source wavefield** models the seismic source (in this case, teleseismic earthquakes, as opposed to the near-offset impulsive sources of industry). For teleseismic sources, the wavefield can be approximated as a plane wave, which can be constructed given information about the incidence angles of the arriving teleseism.

2. The **receiver wavefield** contains the scattered coda. The linear array of seismographs sample this wavefield at z=0 and at discrete x locations. The recorded data, then, serve as a boundary condition on the receiver wavefield. Additionally, the receiver wavefield contains the source wavefield.

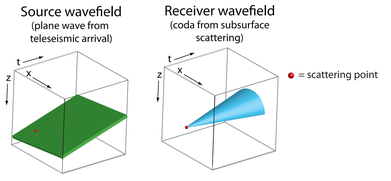

The process of determining the two wavefields is called **wavefield reconstruction** and simulates wave propagation. The process requires a velocity model and an appropriate wave equation. The source wavefield is determined by stepping a plane-wave arrival forward in time through the velocity model. Determining the receiver wavefield requires stepping backward in time; in reality this wavefield is determined using the principle of reciprocity - the receivers are treated as sources and the recorded data as the source signals.

What data are used?

Seismic reflection studies utilize only back-scattered (reflected) *P*-wave energy (Figure **a**), and receiver functions utilize only forward-scattered (transmitted) *P* to *S* conversions (Figure **b**). WEM utilizes *both* forward- and back-scattered energy from *both* *P* and *S* phases (Figures **b** and **c**), and therefore exploits information in the recorded data that is otherwise regarded as noise.

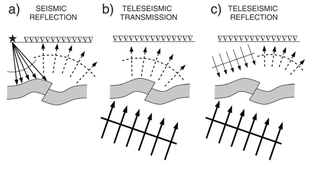

from Bostock et al. 2001

Existing teleseismic imaging approaches

Receiver functions

Probably the most prevalent approach to imaging with teleseismic data has been to convert receiver functions (RFs) from time to depth using a velocity model. This approach can be improved upon with stacking, usually in a CCP sense (e.g. Schulte-Pelkum et al., 2005, Hetenyi, 2007), and optionally migrating. One limitation of this approach is its utilization of only forward-scattered *P* to *S* energy.

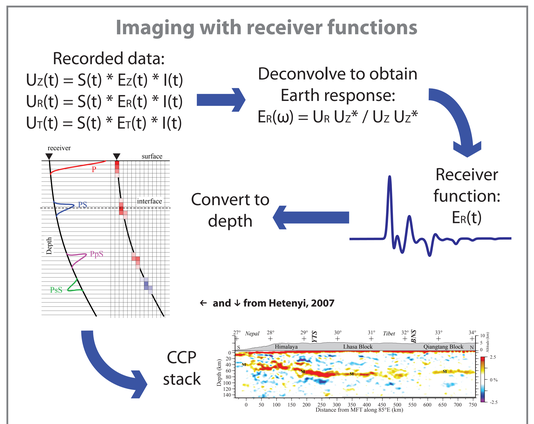

"Deconvolve, then convert to depth"

Inversion of scattered teleseismic waves

A technique upon which this work is based, and which was used to generate the widely-reproduced images of the Cascadia subduction zone, is the inversion of scattered teleseismic waves (Bostock et al., 2001, Rondenay et al., 2001, Bostock et al., 2002). Scattering of teleseismic energy into *P* wave coda can be posed as a forward problem, and the associated inverse problem, utilizing the Radon transform as a back projection operator, generates images of elastic properties using the recorded coda.

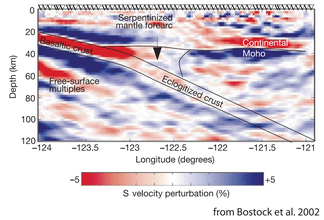

from Bostock et al. 2002

Application of WEM to telesesimic data

How is an image obtained?

The two wavefields created during **wavefield reconstruction** are cross-correlated based on an **imaging condition** of Claerbout (1971) which asserts that source and receiver wavefields are spatially collocated at scattering points (for forward-scattered energy) or reflectors (for backward-scattered energy).

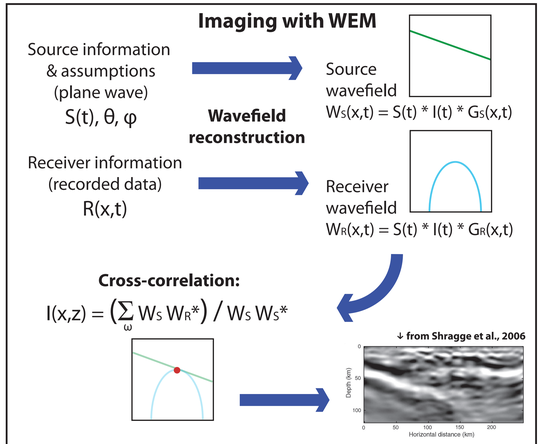

"Propagate to depth, then correlate"

Processing parameters

- Linearly increasing velocity model based on surface wave dispersion (Caldwell et al., 2009). Velocity model is 2.5D and thus assumes constant along-strike velocities.
- Only forward-scattered P-P considered thus far.
- "Interferometric" approach is used in which the source wavefield is not created separately, but rather the receiver wavefield is used as the source wavefield, since the source function is contained in the recorded data.

Data Set

- Nineteen 3-component broadband stations, ~10km spacing, Guralp 3T and 3ESP sensors.
- 452 events of $M_w > 5.0$ and delta 30°-100° recorded between Oct 2005 and Oct 2006.
- Collected by India's National Geophysical Research Institute (NGRI).
- Array crosses the surface expressions of several major features in the Himalayan thrust belt: from south to north, the Main Frontal Thrust (MFT), Main Boundary Thrust (MBT), Main Central Thrust (MCT) and the South Tibetan Detachment (STD).

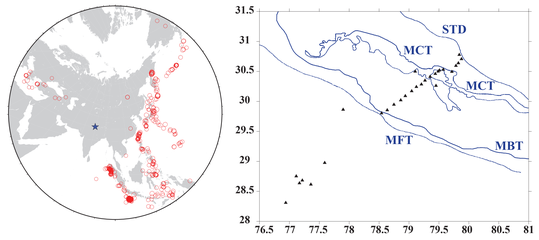

Preliminary Results

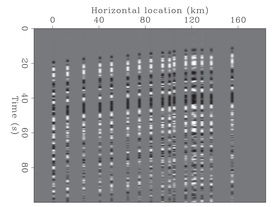

Sample data record for a M_w 7.6 event at 22 km depth in Kamchatka showing consistent reflected energy. Horizontal locations are distances from the MFT.

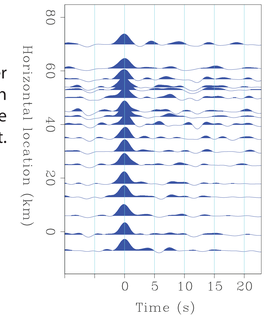

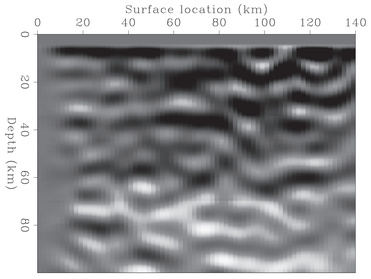

Wave-equation migration image (forward-scattered *P-P*) for same event.

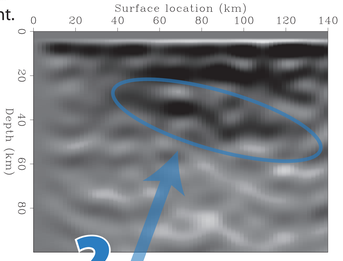

Stack of nine high-quality *P-P* WEM images from nine events, possibly imaging the Main Himalayan Thrust.

Preliminary results suggest that these data may be capable of generating interpretable images using wave-equation migration. In addition to potentially offering new insights into the structure of the Himalayan thrust belt, this has implications for the application of WEM to other broadband arrays with similar station density.

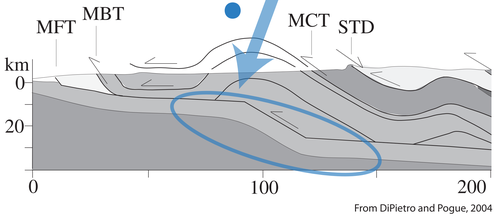

From DiPietro and Pogue, 2004

References

Bostock, M. G., R. D. Hyndman, S. Rondenay, and S. M. Peacock (2002), An inverted continental Moho and serpentinization of the forearc mantle, Nature, 417(6888), 536-538.

Bostock, M. G., S. Rondenay, and J. Shragge (2001), Multiparameter two-dimensional inversion of scattered teleseismic body waves 1. Theory for oblique incidence, Journal of Geophysical Research, 106(B12), pp. 30,771–30,782.

Caldwell, W. B., S. L. Klemperer, S. S. Rai, and J. F. Lawrence (2009), Partial melt in the upper-middle crust of the northwest Himalaya revealed by Rayleigh wave dispersion, Tectonophysics, In Press, doi:10.1016/j.tecto.2009.01.013.

Claerbout, J. F. (1971), Toward a unified theory of reflector mapping, Geophysics, 36(3), 467-481.

DiPietro, J. A., and K. R. Pogue (2004), Tectonostratigraphic subdivisions of the Himalaya: A view from the west, Tectonics, 23, TC5001.

Hetenyi, G. (2007), Evolution of deformation of the Himalayan prism: from imaging to modelling, PhD Thesis.

Rondenay, S., M. G. Bostock, and J. Shragge (2001), Multiparameter two-dimensional inversion of scattered teleseismic body waves 3. Application to the Cascadia 1993 data set, Journal of Geophysical Research, 106(B12), 30,795-30,807.

Sava, P., and S. J. Hill (2009), Overview and classification of wavefield seismic imaging methods, The Leading Edge, 28(2), 170-183.

Schulte-Pelkum, V., G. Monsalve, A. Sheehan, M. R. Pandey, S. Sapkota, R. Bilham, and F. Wu (2005), Imaging the Indian subcontinent beneath the Himalaya, Nature, 435(7046), 1222-1225.

Shragge, J., B. Artman, and C. Wilson (2006), Teleseismic shot-profile migration, Geophysics, 71(4), SI221-SI229.